

Critical behavior of the Higgs- and Goldstone-mass gaps for the two-dimensional $S = 1$ XY model

Yoshihiro Nishiyama

*Department of Physics, Faculty of Science, Okayama University, Okayama 700-8530,
Japan*

Abstract

Spectral properties for the two-dimensional quantum $S = 1$ XY model were investigated with the exact diagonalization method. In the symmetry-broken phase, there appear the massive Higgs and massless Goldstone excitations, which correspond to the longitudinal and transverse modes of the spontaneous magnetic moment, respectively. The former excitation branch is embedded in the continuum of the latter, and little attention has been paid to the details, particularly, in proximity to the critical point. The finite-size-scaling behavior is improved by extending the interaction parameters. An analysis of the critical amplitude ratio for these mass gaps is made.

Keywords:

75.10.Jm 75.40.Mg 05.50.+q , 05.70.Jk

1. Introduction

In the symmetry-broken phase, the $O(2)$ -symmetric system, such as the XY model, exhibits a massless Goldstone excitation, which corresponds to the transverse modulation of the magnetic moment. On the one hand, the longitudinal mode, namely, the Higgs excitation, is massive, embedded in the

continuum of the former; see Ref. [1] for a review. The O(2)- [equivalently, U(1)-] symmetric system is ubiquitous in nature, and such a characteristic spectrum has been observed for a variety of substances [2, 3, 4, 5, 6, 7, 8, 9, 10, 11]. The perturbation field (experimental probe) should retain the O(2) (axial) symmetry [1, 12, 13, 14, 15]; otherwise, the contribution from the Goldstone excitations smears out the Higgs-mode branch [16, 17, 18, 19]. (For instance, the chemical-potential modulation for the bosonic system does not conflict with the symmetry.)

Recent studies [20, 21] shed light on a universal character of the spectrum in proximity to the phase transition, especially, in $(2 + 1)$ dimensions; it would be intriguing that the spectral property is also under the reign of universality. In $(3 + 1)$ dimensions, the criticality is described simply by the Ginzburg-Landau theory (Gaussian fixed point). On the contrary, in $(2 + 1)$ dimensions, the spectral property is non-perturbative by nature. In particular, a universal amplitude ratio for the mass gaps [see Eq. (1) mentioned afterward] is arousing much attention recently.

In this paper, we investigate the two-dimensional quantum $S = 1$ -spin XY model (2) with the exact diagonalization method. The method enables us to calculate the low-lying level indexed by quantum numbers. In order to suppress corrections to scaling, we incorporate various types of interaction parameters in addition to the ordinary nearest-neighbor ferromagnetic interaction J_{NN} . Thereby, we investigate the universality for the critical amplitude ratio

$$m_H/\Delta \equiv \frac{m_H(J_{NN})}{m_G(2J_{NN}^* - J_{NN})}, \quad (1)$$

with the Higgs mass m_H , the Goldstone mass m_G , and the reflected gap

$\Delta = m_G(2J_{NN}^* - J_{NN})$ with respect to the critical point J_{NN}^* ; technical details and underlying physics are explained in the next section. The amplitude ratio has been estimated as $m_H/\Delta = 2.1(3)$ [22, 23] and $3.3(8)$ [24] by means of the (quantum) Monte Carlo method. According to the recent elaborated renormalization-group analyses, the ratio was estimated as 2.4 [25], 2.2 [26], and 1.67 [27].

To be specific, we present the Hamiltonian for the $S = 1$ XY model [28]

$$\begin{aligned} \mathcal{H} = & -J_{NN} \sum_{\langle ij \rangle} (S_i^x S_j^x + S_i^y S_j^y) - J_{NNN} \sum_{\langle\langle ij \rangle\rangle} (S_i^x S_j^x + S_i^y S_j^y) \\ & + D_{\square} \sum_{[ijkl]} (S_i^z + S_j^z + S_k^z + S_l^z)^2 + D \sum_i (S_i^z)^2. \end{aligned} \quad (2)$$

Here, the quantum $S = 1$ -spin operator \mathbf{S}_i is placed at each square-lattice point i . The summations, $\sum_{\langle ij \rangle}$, $\sum_{\langle\langle ij \rangle\rangle}$, and $\sum_{[ijkl]}$, run over all possible nearest-neighbor, next-nearest-neighbor, and plaquette spins, respectively. The parameters $(J_{NN}, J_{NNN}, D_{\square})$ are the corresponding coupling constants. The parameter D denotes the single-ion anisotropy. We survey the coupling-constant subspace

$$(J_{NN}, J_{NNN}, D_{\square}, D) = (J_{NN}, J_{NNN}^* J_{NN} / J_{NN}^*, D_{\square}^*, D^*), \quad (3)$$

parameterized by J_{NN} . At $J_{NN} = J_{NN}^*$, the system undergoes a phase transition; a schematic phase diagram is presented in Fig. 1. Here, the critical point

$$(J_{NN}^*, J_{NNN}^*, D_{\square}^*, D^*) = (0.158242810160, 0.058561393564, 0.10035104389, 0.957), \quad (4)$$

was adjusted [28] to an IR fixed point with almost eliminated irrelevant interactions; that is, the coupling constants $(J_{NN}^*, J_{NNN}^*, D_{\square}^*)$ were determined

through an approximative real-space renormalization group, and the remaining one D^* was finely tuned via the conventional finite-size-scaling analysis. As shown in Eq. (2), the $S = 1$ -spin model allows us to incorporate various interactions such as the single-ion anisotropy, with which one is able to realize the XY -paramagnetic phase transition. In this sense, the extension of the magnetic moment to $S = 1$ is essential in our study.

The rest of this paper is organized as follows. In Sec. 2, we present the simulation results. Technical details are explained as well. In Sec. 3, we address the summary and discussions.

2. Numerical results

In this section, we present the simulation results. To begin with, we explain the simulation technique.

2.1. Simulation algorithm

In this section, we explain the simulation algorithm. As mentioned in Introduction, the XY model (2) was simulated with the exact diagonalization method. We implemented the screw-boundary condition [29] in order to treat a variety of system sizes $N = 10, 12, \dots, 22$ (N : number of constituent spins) systematically; note that conventionally, the system size N is restricted within $N = 9, 16, \dots$. We adopt the algorithm presented in Sec. II of Ref. [28]. The linear dimension L is given by $L = \sqrt{N}$; note that the N spins constitute a rectangular cluster.

Thereby, we evaluated the mass gaps m_H and m_G via the following scheme. The exact diagonalization method yields the low-lying energy levels $E_0 < E_1 < E_2 < \dots$ explicitly. Each level $E_i(k, S_{tot}^z)$ is specified by the

momentum k and the perpendicular magnetic moment S_{tot}^z ; in practice, the numerical diagonalization was performed within the subspace (k, S_{tot}^z) . The Higgs- and Goldstone-mass gaps are characterized by

$$m_H = E_1(0, 0) - E_0(0, 0), \quad (5)$$

and

$$m_G = E_0(0, 1) - E_0(0, 0), \quad (6)$$

respectively. The reflected gap Δ with respect to the critical point J_{NN}^* is calculated by $\Delta = m_G(2J_{NN}^* - J_{NN})$. The gap $m_G(\Delta)$ becomes massive in the paramagnetic (XY) phase $J_{NN} < J_{NN}^*$ ($J_{NN} > J_{NN}^*$), and hence, the ratio m_H/Δ makes sense in the XY phase. The gap $\Delta > 0$ is interpreted as the insulator gap through regarding the ladder operators S_i^\pm as the bosonic creation-annihilation operators.

2.2. Scaling analyses of $m_{H,G}$

In this section, we investigate the scaling behaviors for the mass gaps m_H (5) and m_G (6).

In Fig. 2, we present the scaled Higgs gap Lm_H for the nearest-neighbor ferromagnetic interaction J_{NN} and various system sizes $N = 10, 12, \dots, 22$ ($L = \sqrt{N}$). The data merge around $J_{NN} \approx 0.15$, indicating an onset of criticality; note that the scaled energy gap should be scale-invariant at the critical point. The location of the critical point is consistent with Eq. (4). The Higgs gap m_H appears to open in both the paramagnetic ($J_{NN} < J_{NN}^*$) and XY ($J_{NN} > J_{NN}^*$) phases; the latter case is our main concern, as mentioned in Introduction.

In Fig. 3, we present the scaled Goldstone gap Lm_G for various J_{NN} and $N = 10, 12, \dots, 22$. The data indicate an onset of criticality around $J_{NN} \approx 0.15$. The Goldstone gap closes in the XY phase, while it opens in the paramagnetic phase. The latter gap is interpreted as the (bosonic) insulator gap Δ , setting a fundamental energy scale in this domain; actually, the transition is interpreted as the superfluid-insulator transition [21]. Hence, the ratio m_H/Δ , Eq. (1), makes sense in the XY phase, and the criticality is investigated in the next section.

In Fig. 4, we present the scaling plot, $(J_{NN} - J_{NN}^*)L^{1/\nu} - Lm_H$, for various system sizes $N = 10, 12, \dots, 22$. Here, the scaling parameters are set to $J_{NN}^* = 0.158242810160$ [Eq. (4)] and $\nu = 0.6717$ [30, 31]. The data appear to collapse into a scaling curve satisfactorily. Similarly, in Fig. 5, we present the scaling plot, $(J_{NN} - J_{NN}^*)L^{1/\nu} - Lm_G$, for various system sizes $N = 10, 12, \dots, 22$; the scaling parameters are the same as those of Fig. 4.

We address a few remarks. First, the data in Figs. 4 and 5 collapse into the scaling curves satisfactorily. Such a feature indicates that corrections to scaling are almost negligible owing to the fine adjustment [28] of the coupling constants to Eq. (4). Because the tractable system size with the exact diagonalization method is severely restricted, it is significant to accelerate the convergence to the scaling limit. Second, the scaling parameters, J_{NN}^* and ν , are taken from the literatures, Refs. [28] and [30], respectively. That is, there are no adjustable *ad hoc* parameters in the present scaling analyses. Last, as demonstrated in Figs. 2 and 3, both mass gaps $m_{H,G}$ possess an identical scaling dimension. Hence, the amplitude ratio (1) makes sense, and the criticality is explored in the next section.

2.3. Analysis of the amplitude ratio m_H/Δ

In this section, encouraged by the findings in Sec. 2.2, we turn to the analysis of the amplitude ratio m_H/Δ , Eq. (1).

In Fig. 6, we present the scaling plot, $(J_{NN} - J_{NN}^*)L^{1/\nu} - m_H/\Delta$, for $N = 10, 12, \dots, 22$; here, the scaling parameters, J_{NN}^* and ν , are the same as those of Fig. 4. In the XY phase, $J_{NN} - J_{NN}^* > 0$, the amplitude ratio exhibits a plateau for an appreciable range of J_{NN} . Such a feature clearly indicates that the amplitude ratio is a universal constant in this domain.

Upon close inspection, the plateaux in Fig. 6 are curved concavely. The shallow bottom locates at $J_{NN} = \bar{J}_{NN}$, satisfying $\partial_{J_{NN}}(m_H/\Delta)|_{J_{NN}=\bar{J}_{NN}} = 0$ for each system size N . We regard the bottom height

$$m_H/\Delta|_{J_{NN}=\bar{J}_{NN}}, \quad (7)$$

as an indicator for m_H/Δ . The amplitude ratio (7) is plotted for $1/L^2$ [$N(=L^2) = 10, 12, \dots, 22$] in Fig. 7. The least-squares fit to the data yields an estimate $m_H/\Delta = 2.119(13)$ in the thermodynamic limit $L \rightarrow \infty$. As a reference, a similar analysis was performed with the abscissa scale replaced with $1/L$, and we arrived at $m_H/\Delta = 1.923(17)$. The discrepancy ≈ 0.2 between these estimates appears to dominate the least-squares-fit error ≈ 0.02 , and the discrepancy may indicate an ambiguity as to the extrapolation (systematic error). Regarding it as a possible systematic error, we estimate the amplitude ratio as

$$m_H/\Delta = 2.1(2). \quad (8)$$

A comment may be in order, the series of data in Fig. 7 appear to be oscillatory; actually, we observe a slight bump around $N(=L^2) \approx 16$. Such

an oscillatory behavior is an artifact of the screw-boundary condition [29], rendering an ambiguity as to the extrapolation to $L \rightarrow \infty$. The ambiguity appears to be bounded by the above-mentioned error margin, which is estimated by performing two independent extrapolation schemes.

3. Summary and discussions

The critical behavior of $m_{H,G}$ was investigated for the two-dimensional quantum $S = 1$ XY model (2) by means of the numerical diagonalization method [29, 28]. The interaction parameters were adjusted to Eq. (3) in order to suppress corrections to scaling [28]. As a consequence, the data (Figs. 4 and 5) collapse into the scaling curves satisfactorily, indicating that the data already enter the scaling regime. Thereby, we confirm a universal character for the mass-gap ratio (Fig. 6), and estimate the amplitude ratio as $m_H/\Delta = 2.1(2)$.

As mentioned in Introduction, the amplitude ratio has been estimated with the (quantum) Monte Carlo method, $m_H/\Delta = 2.1(3)$ [22, 23] and $3.3(8)$ [24], as well as the renormalization-group approaches, 2.4 [25], 2.2 [26], and 1.67 [27]. According to the Ginzburg-Landau (mean-field) theory, the amplitude ratio should be $m_H/\Delta = \sqrt{2}$. Clearly, the spectral property reveals a notable deviation from that anticipated from the mean-field theory; the Ising counterpart was studied in Ref. [32]. In this respect, detailed analyses of other spectral properties such as the AC conductivity [23, 33] would be desirable. A progress toward this direction is left for the future study.

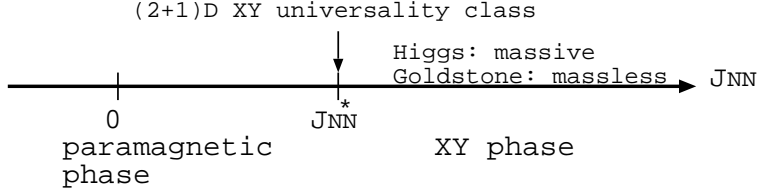


Figure 1: A schematic phase diagram for the two-dimensional $S = 1$ XY model (2) is presented; here, the parameter space is described by the formula (3). As the nearest-neighbor ferromagnetic interaction J_{NN} increases, a phase transition from the paramagnetic phase to the XY phase occurs. The critical behaviors for the Higgs- and Goldstone-mass gaps are the main concern.

Acknowledgment

This work was supported by a Grant-in-Aid for Scientific Research (C) from Japan Society for the Promotion of Science (Grant No. 25400402).

References

- [1] D. Pekker and C.M. Varma, Annual Rev. Condens. Matter Phys. **6** (2015) 269.
- [2] Ch. Rüegg, B. Normand, M. Matsumoto, A. Furrer, D. F. McMorrow, K. W. Krämer, H. -U. Güdel, S. N. Gvasaliya, H. Mutka, and M. Boehm, Phys. Rev. Lett. **100** (2008) 205701.
- [3] U. Bissbort, S. Götze, Y. Li, J. Heinze, J. S. Krauser, M. Weinberg, C. Becker, K. Sengstock, and W. Hofstetter, Phys. Rev. Lett. **106** (2011) 205303.

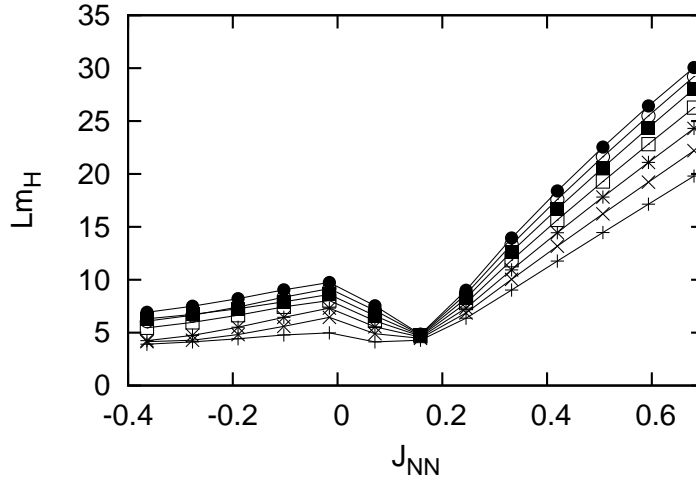


Figure 2: The scaled Higgs mass Lm_H is plotted for various J_{NN} and the system sizes of (+) $N(=L^2)=10$, (\times) 12, (*) 14, (\square) 16, (\blacksquare) 18, (\circ) 20, and (\bullet) 22. The scale-invariant point, $J_{NN}^* \approx 0.15$, indicates the location of the critical point. The Higgs gap opens in the XY phase, $J_{NN} > J_{NN}^*$.

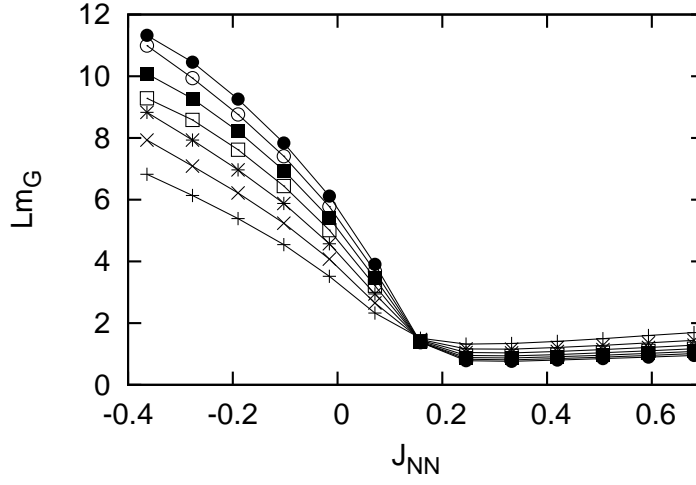


Figure 3: The scaled Goldstone mass Lm_G is plotted for various J_{NN} and the system sizes of (+) $N = 10$, (\times) 12 , ($*$) 14 , (\square) 16 , (\blacksquare) 18 , (\circ) 20 , and (\bullet) 22 . The intersection point of the curves, $J_{NN}^* \approx 0.15$, indicates the location of the critical point. The Goldstone excitation is massless in the XY phase, $J_{NN} > J_{NN}^*$. The mass $\Delta > 0$ in the paramagnetic phase is interpreted as the insulator gap in the boson language.

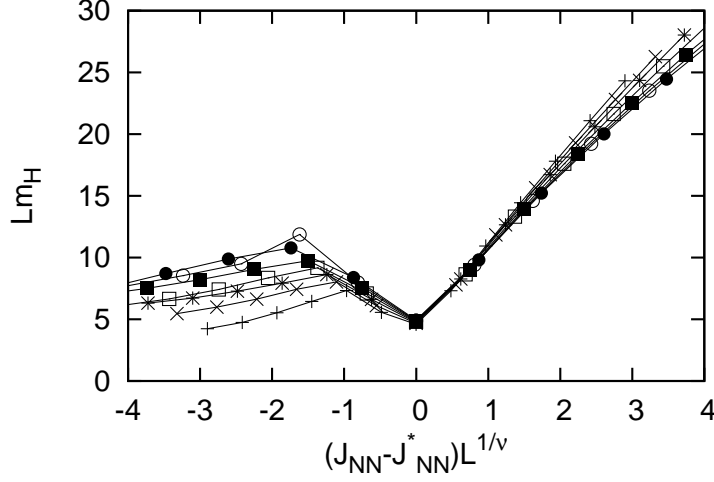


Figure 4: The scaling plot, $(J_{NN} - J_{NN}^*)L^{1/\nu} - Lm_H$, is presented for the system sizes (+) $N = 10$, (\times) 12, (*) 14, (\square) 16, (\blacksquare) 18, (\circ) 20, and (\bullet) 22. The scaling parameters are set to $J_{NN}^* = 0.158242810160$ [28] and $\nu = 0.6717$ [30].

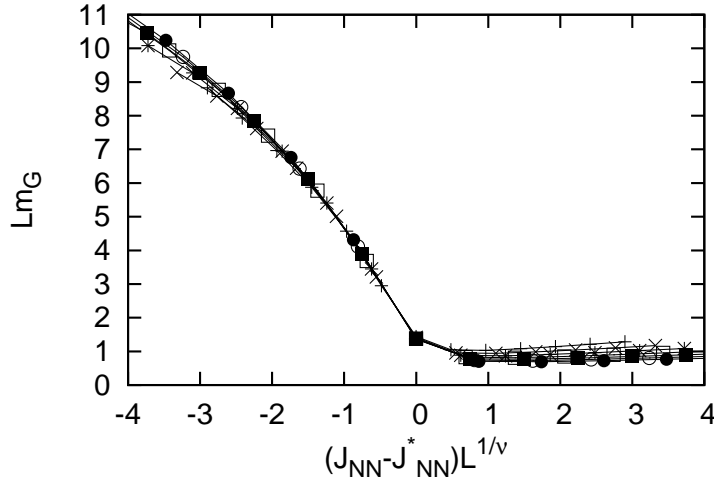


Figure 5: The scaling plot, $(J_{NN} - J_{NN}^*)L^{1/\nu} - Lm_G$, is presented for the system sizes (+) $N = 10$, (\times) 12, (*) 14, (\square) 16, (\blacksquare) 18, (\circ) 20, and (\bullet) 22. The scaling parameters, J_{NN}^* and ν , are the same as those of Fig. 4.

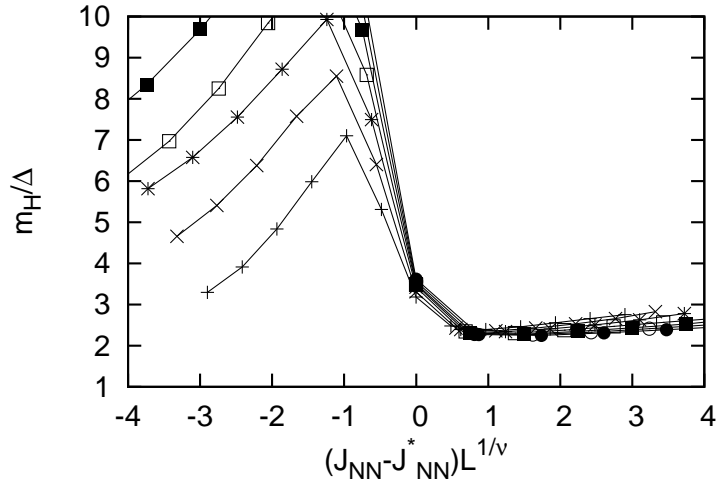


Figure 6: The scaling plot, $(J_{NN} - J_{NN}^*)L^{1/\nu} - m_H/\Delta$, is presented for the system sizes $(+)$ $N = 10$, (\times) 12, $(*)$ 14, (\square) 16, (\blacksquare) 18, (\circ) 20, and (\bullet) 22. The scaling parameters, J_{NN}^* and ν , are the same as those of Fig. 4. A plateau appears in the XY phase, indicating a universal character of the amplitude ratio.

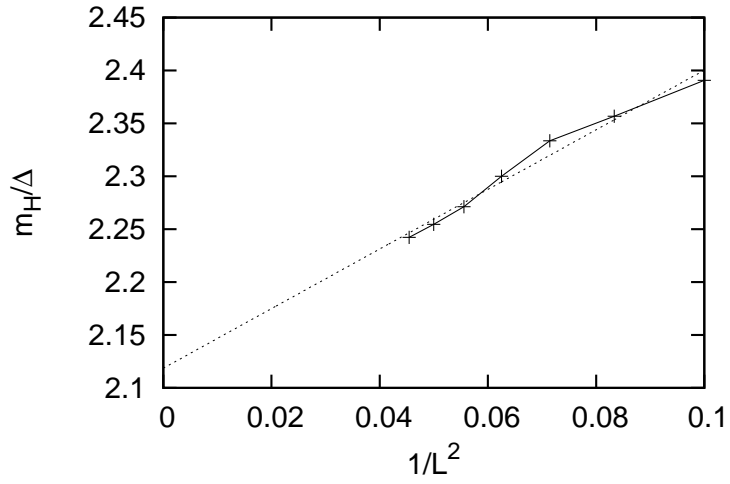


Figure 7: The mass-gap amplitude ratio m_H/Δ (7) is plotted for $1/L^2$ ($N = 10, 12, \dots, 22$). The least-squares fit to the data yields $m_H/\Delta = 2.119(13)$ in the thermodynamic limit $L \rightarrow \infty$. A possible extrapolation error is considered in the text. An oscillatory deviation (slight bump around $L^2 \approx 16$) is an artifact of the screw-boundary condition [29].

- [4] M. Endres, T. Fukuhara, D. Pekker, M. Cheneau, P. Schauß, C. Gross, E. Demler, S. Kuhrand, and I. Bloch, *Nature* **487** (2012) 454.
- [5] J. Demsar, K. Biljaković, and D. Mihailovic, *Phys. Rev. Lett.* **83** (1999) 800.
- [6] R. Yusupov, T. Mertelj, V. V. Kabanov, S. Brazovskii, P. Kusar, J.-H. Chu, I. R. Fisher and D. Mihailovic, *Nature Phys.* **6** (2010) 681.
- [7] K. B. Lyons, P. A. Fleury, J. P. Remeika, A. S. Cooper, and T. J. Negran, *Phys. Rev. B* **37** (1988) 2353.
- [8] J.B. Parkinson, *J. Phys. C Solid State Phys.* **2** (1969) 2003.
- [9] P. A. Fleury and H. J. Guggenheim, *Phys. Rev. Lett.* **24** (1970) 1346.
- [10] R. J. Elliott and M. F. Thorpe, *J. Phys. C Solid State Phys.* **2** (1969) 1630.
- [11] B. S. Shastry and B. I. Shraiman, *Phys. Rev. Lett.* **65** (1990) 1068.
- [12] N. H. Lindner and A. Auerbach, *Phys. Rev. B* **81** (2010) 054512.
- [13] D. Podolsky, A. Auerbach, and D. P. Arovas, *Phys. Rev. B* **84** (2011) 174522.
- [14] S. D. Huber, E. Altman, H. P. Büchler, and G. Blatter, *Phys. Rev. B* **75** (2007) 085106.
- [15] S. D. Huber, B. Theiler, E. Altman, and G. Blatter, *Phys. Rev. Lett.* **100** (2008) 050404.

- [16] A. V. Chubukov, S. Sachdev, and J. Ye, Phys. Rev. B **49** (1994) 11919.
- [17] S. Sachdev, Phys. Rev. B **59** (1999) 14054.
- [18] W. Zwirger, Phys. Rev. Lett. **92** (2004) 027203.
- [19] N. Dupuis, Phys. Rev. A **80** (2009) 043627.
- [20] D. Podolsky and S. Sachdev, Phys. Rev. B **86** (2012) 054508.
- [21] L. Pollet and N. Prokof'ev, Phys. Rev. Lett. **109** (2012) 010401.
- [22] S. Gazit, D. Podolsky, and A. Auerbach, Phys. Rev. Lett. **110** (2013) 140401.
- [23] S. Gazit, D. Podolsky, A. Auerbach, and D. P. Arovas, Phys. Rev. B **88** (2013) 235108.
- [24] K. Chen, L. Liu, Y. Deng, L. Pollet, and N. Prokof'ev, Phys. Rev. Lett. **110** (2013) 170403.
- [25] A. Rançon and N. Dupuis, Phys. Rev. B **89** (2014) 180501.
- [26] F. Rose, F. Léonard and N. Dupuis, Phys. Rev. B **91** (2015) 224501.
- [27] Y. T. Katan and D. Podolsky, Phys. Rev. B **91** (2015) 075132.
- [28] Y. Nishiyama, Phys. Rev. E **78** (2008) 021135.
- [29] M.A. Novotny, J. Appl. Phys. **67** (1990) 5448.
- [30] M. Campostrini, M. Hasenbusch, A. Pelissetto, and E. Vicari, Phys. Rev. B **74** (2006) 144506.

- [31] E. Burovski, J. Machta, N. Prokof'ev, and B. Svistunov, Phys. Rev. B **74** (2006) 132502.
- [32] S. Dusuel, M. Kamfor, K.P. Schmidt, R. Thomale, and J. Vidal, Phys. Rev. B **81** (2010) 064412.
- [33] K. Chen, L. Liu, Y. Deng, L. Pollet, and N. Prokof'ev, Phys. Rev. Lett. **112** (2014) 030402.